Optical second-harmonic generation during switching in a ferroelectric liquid-crystal cell

I. Drevenšek Olenik,[1] R. Torre,[2] and M. Čopič[1,*]
[1]J. Stefan Institute, University of Ljubljana, Jamova 39, 61111 Ljubljana, Slovenia
[2]European Laboratory for Nonlinear Spectroscopy, Largo Enrico Fermi 2, 50125 Florence, Italy
(Received 15 December 1993)

We report measurements of the temporal dependence of the second-harmonic generation from a 50 μm thick homeotropically aligned cell of ferroelectric liquid crystal (SCE9) (British Drug House, Ltd.) exposed to a symmetric square wave form electric field. The field switches the molecular configuration between the two unwound states with the director on the opposite positions of the tilt cone. The response of the second-harmonic signal measured in the phase matching geometry for one of these equilibrium states shows that a complete switching process takes several seconds. In experimental geometries away from the equilibrium phase matching geometry a strong transient second-harmonic signal is observed during the switching. It corresponds to the transient realization of the phase matching condition related to the intermediate molecular configurations. The study of this effect provides a precise time resolved monitoring of the molecular dynamics during the switching. Our results show that the director reorientation in a hometropic cell goes on within numerous domains of a size much smaller than the optical wavelength. On the basis of this assumption the temporal dependence of the director reorientation within the domains is calculated.

PACS number(s): 61.30.−v, 42.65.Ky, 78.20.Jq, 42.79.Kr

I. INTRODUCTION

The manifold applications of ferroelectric liquid crystals (FLC) in fast electro-optic devices have stimulated several studies of the switching process in FLC cells. Most of the studies have considered optical transmittance changes in thin (~ 1 μm) surface stabilized cells (SSFLC) placed between crossed polarizers and exposed to alternating electric field [1–5]. In SSFLC cells the helical structure of the smectic-C^* (Sm-C^*) phase is suppressed by the surface [6]. The theoretical models of the switching process show that in many cases a spatial inhomogeneity of the molecular reorientation has to be taken into account to adequately explain the observed features [7–12]. Some studies were performed also on thicker (~ 10 μm) planarly aligned cells (smectic layers perpendicular to the surface) where the formation of the Sm-C^* helix plays an important role [13–15]. Due to this property the electro-optic response becomes very slow and complicated and is at present not theoretically described. In contrast to planar cells the studies of the switching process in homeotropically aligned cells (smectic layers parallel to the surface) have been very rare. Ozaki and co-workers have reported millisecond transmittance variation in a 13 μm thick homeotropic FLC cell exposed to a square wave form field [16,17]. They also mentioned a possibility for application of this type of cells for modulation of the optical second-harmonic generation.

The lack of inversion symmetry in the Sm-C^* phase allows optical second-harmonic generation (SHG) in this mesophase. The SHG is pronounced only in cells with the unwound helix [18,19]. In this respect the unwinding by the surface coupling is not very appropriate because of the limited thickness of the SSFLC cells which results in a low output power of the second-harmonic beam. More suitable thick cells are usually unwound by the application of an external electric field above some critical magnitude E_c. To obtain an efficient SHG from a thick cell the phase matching (PM) condition has to be realized. The realization of PM condition, which compensates the material color dispersion, is achieved by the use of the FLC birefringence. The PM geometry is easily established in a homeotropically aligned cell when the cell is rotated with respect to the incident beam around the direction of the external field [20,21]. The width of the PM peak in 100 μm thick cells is usually only a few degrees [22]. Such a narrow peak is very sensitive to any changes of molecular configuration within the cell and its investigation thus provides a possibility to follow the molecular reorientation during the switching process.

The dynamic response of the SHG signal on a step field and on an asymmetric square wave form field applied to the homeotropically aligned FLC cells were studied recently [23,24]. These studies provide information on the dynamics of the winding and unwinding process of the Sm-C^* helix. In this paper we present the results on the SHG response of the homeotropically aligned FLC cell exposed to a symmetric square wave form field. The field is varied in frequency and amplitude. This field switches the molecular configuration between the two unwound states with the opposite position of the director on the tilt cone. We studied also the angular dependence of the modulated SHG signal which gives the PM profiles related to the intermediate molecular configurations realized during the switching. From this study we deduce the temporal dependence of the director reorientation which is calculated assuming a multidomain switching process.

*Also at Department of Physics, University of Ljubljana, Jadranska 19, 61111 Ljubljana, Slovenia.

 ©1994 The American Physical Society

II. EXPERIMENT

The compound used in our investigation was a commercial British Drug House mixture SCE9. It has a room temperature Sm-C^* phase with the tilt angle θ of 20.5° at 20 °C. The SCE9 is very appropriate for investigation of the dynamic SHG response due to its high spontaneous polarization ($P_s = 33.6$ nC/cm^2 at 20 °C), long helical pitch ($p \approx 15$ μm) and high second order nonlinear optical susceptibility $\chi^{(2)}$. Due to these properties efficient SHG modulation is achieved by low electric fields. The components of the nonlinear susceptibility χ_{ijk} and the color dispersion of the refractive index of SCE9 have been previously determined by Liu *et al.* [25]. This allowed us to concentrate directly on the dynamic properties of the SHG in this material. A homeotropically aligned cell was prepared using silane (DMOAP) coated glass plates separated by two 50 μm thick Mylar spacers. One of the glass plates was covered also by two stripes of conducting indium tin oxide (ITO) layer which served as electrodes to provide electric field parallel to the glass surfaces. The gap between the electrodes was 1.4 mm.

The fundamental light source in the experimental setup was a Q-switched Nd-YLF laser operating at a repetition rate of 1 kHz. It provided 7 ns long light pulses with the 1.046 μm wavelength. The average power of the outgoing beam was 150 mW. The beam passed a polarizer and a visible-cut filter and was then focused on the sample by a cylindrical lens with a focal length of 500 mm. The laser spot size on the sample was around 0.6 mm×0.1 mm with the long axis parallel to the electrodes. The focusing with the cylindrical lens was used to increase the homogeneity of the external field within the region of the laser spot. The second-harmonic beam was separated from the fundamental beam by a grating spectrometer and detected by a photomultiplier. The output from the photomultiplier was connected to a gated integrator synchronized with the laser. The integrated signal was monitored on a digital oscilloscope and was averaged up to 256 times. As there was no synchronization between the laser Q-switched unit and the square wave form field which was applied to the sample and was also triggering the scope, the multiple averaging of the signal provided random sampling, giving an effective time resolution of about 10 μs.

All the measurements were performed at room temperature. The sample was mounted on the rotation stage, which allowed rotation of the sample around the direction of the external field (Fig. 1). This direction is chosen as the y axis of the coordinate system. An unwinding dc field of the magnitude 1570 V/cm was applied to the sample. This field corresponds to the field five times larger than the critical field E_c necessary to unwind the helical structure. The position corresponding to the type I (*ee-o*) PM was found. The type I (*ee-o*) PM is a PM with the fundamental beam polarized as an extraordinary beam and the second-harmonic beam polarized as an ordinary beam. The PM was achieved when the incident angle α of the laser beam with respect to the sample normal was 2.5°. For the applied dc field of −1570 V/cm the PM appeared at $\alpha = -2.5°$. After determination of the PM profile in the dc field the field was changed to the square wave form field.

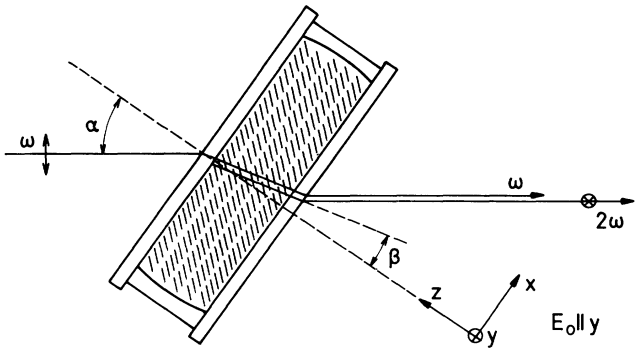

FIG. 1. Experimental geometry.

III. RESULTS

In the first series of measurements we investigated the dependence of the SHG response on the frequency of the modulating field. The amplitude of the applied field was 1570 V/cm. The measurements were performed at $\alpha = 2.5°$. Figure 2 shows the temporal behavior of the second-harmonic power $P_{2\omega}$ at four different frequencies of the modulating field. The temporal dependence of the field is also marked. The field switches the molecular configuration into and out of the PM geometry. At the frequency of 0.05 Hz the temporal behavior of the $P_{2\omega}$ is as expected [Fig. 2(a)]. The orientation of the cell corresponds to the PM direction for the positive dc field and therefore the SHG signal is high when the field is positive and decreases to almost zero when the field is negative. It takes around 5 s for the signal to change between these two dc field determined equilibrium values. At the modulation frequency of 1 Hz the SHG signal decreases [Fig. 2(b)]. The equilibrium values of $P_{2\omega}$ are no longer realized.

A very unusual behavior is observed for the 8.5 Hz modulation [Fig. 2(c)]. At this frequency the situation becomes totally opposite with respect to 0.05 Hz modulation. The SHG signal is very low when the field is positive and is high when the field is negative. An interval of zero signal, about 5 ms long, is noticed just after the field sign is changed. This dip predominates at the modulation frequency of 50 Hz [Fig. 2(d)]. At the frequencies above 100 Hz the SHG is zero all the time.

To explain the behavior of the SHG signal at different frequencies, we measured the angular dependence of $P_{2\omega}$ within the negative field intervals during the 10 Hz modulation and compared it to the angular dependence in the negative dc field of the same magnitude. These angular dependencies are presented in Fig. 3. The data for 10 Hz modulation correspond to the values of $P_{2\omega}$ at the end of the negative field intervals. The typical dc field determined profile of the PM curve remains even during the 10 Hz modulation, but the position of the peak is shifted from $\alpha = -2.5°$ to 4° and the amplitude of the

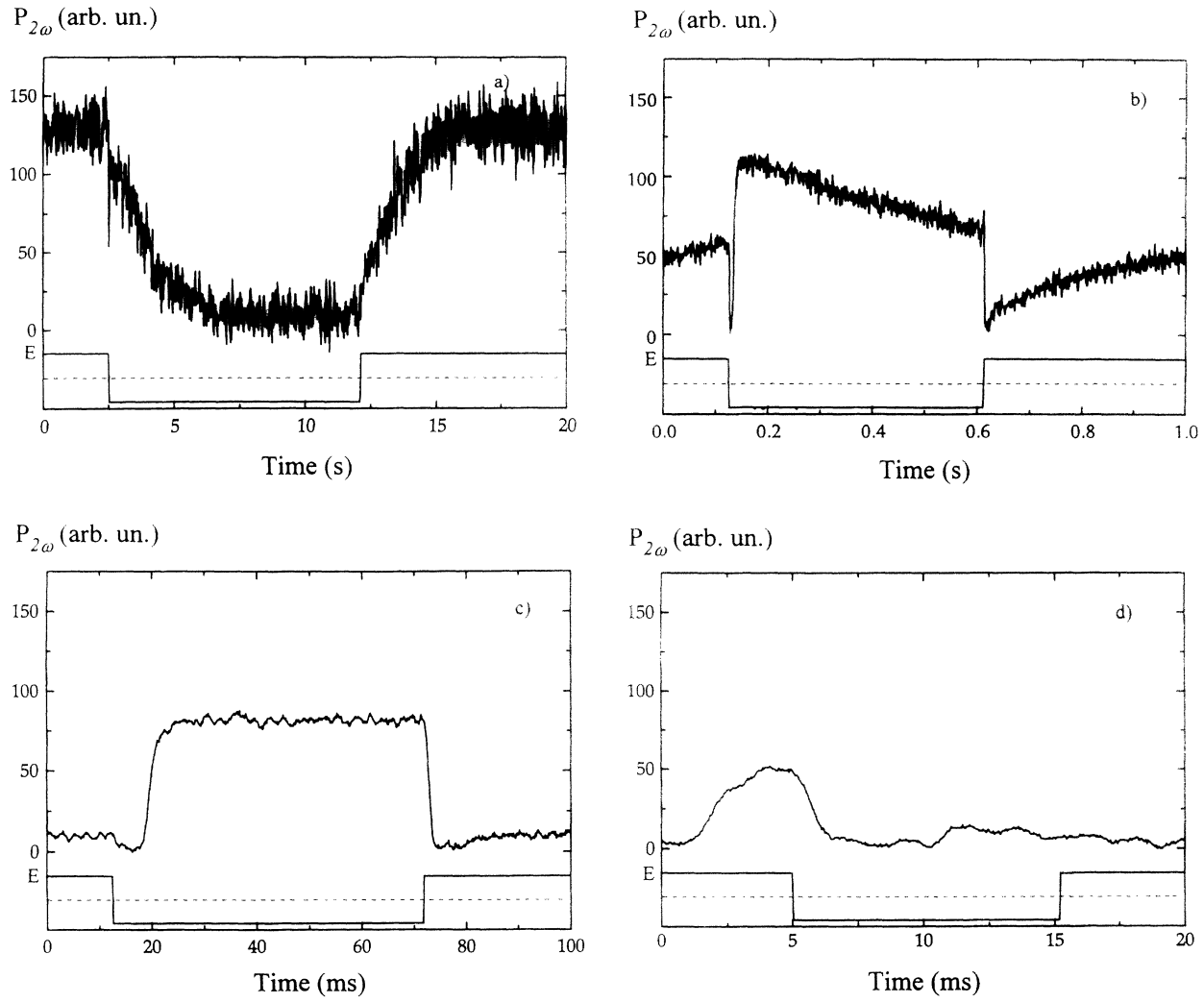

FIG. 2. Temporal dependence of the SHG at different frequencies of the square wave form field: (a) $\nu=0.05$ Hz, (b) $\nu=1$ Hz, (c) $\nu=8.5$ Hz, and (d) $\nu=50$ Hz. Temporal dependence of the field is shown at the bottom of the figures. The dashed line corresponds to zero field.

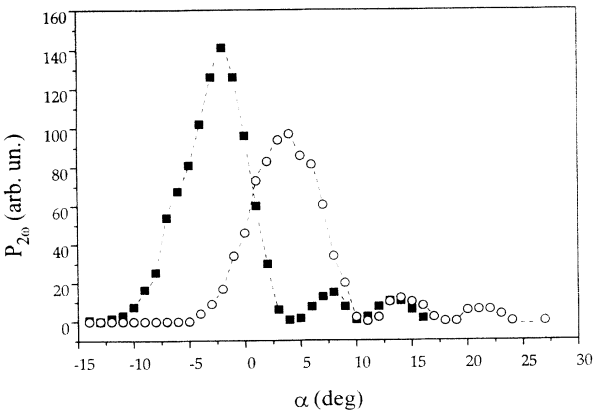

FIG. 3. Angular dependence of the second-harmonic power $P_{2\omega}$ in the negative dc field (squares) and at the end of the negative field intervals of the square wave form field with the frequency of 10 Hz (circles).

peak is decreased. The shift of the PM direction with the frequency explains the different temporal SHG responses observed for 8.5 and 0.05 Hz modulation.

At the incident angles $\alpha<-4°$ and $\alpha>4°$ interesting transient maxima appear in the SHG response during 10 Hz modulation. They are illustrated in Fig. 4, which shows the temporal dependence of $P_{2\omega}$ in different experimental geometries. At $\alpha=7°$ the dependence is similar to what is observed at $\alpha=2.5°$. There is almost no SHG signal in the positive field and a lot of signal in the negative field. But when the cell is rotated to some larger values of α this signal decreases and what remains are only the two short second-harmonic light pulses which appear some delay time τ after the field sign is changed. At α around 30° they disappear too. These transient SHG peaks are linearly polarized along the y axis.

Figure 5 shows the delay time τ of the transient SHG peaks as a function of α. The delay time of the peaks following the + to − sign change decreases with the in-

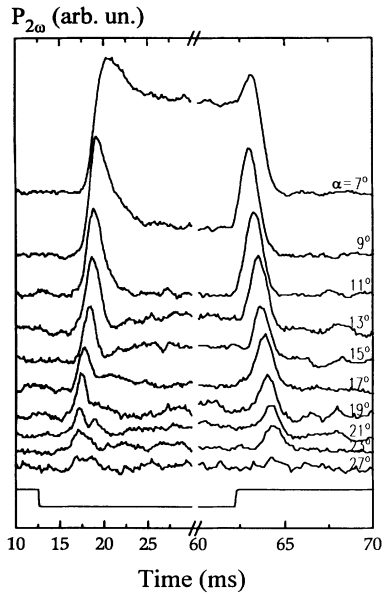

FIG. 4. Temporal dependence of the SHG at different incident angles α of the fundamental beam. The temporal dependence of the field is marked in the bottom of the figure.

creasing α, while the delay time of the peaks following the − to + sign change increases with the increasing α. On the contrary the height of the peaks $P_{2\omega,\max}$ decreases with the increasing α for both kinds of sign changes (Fig. 6).

In the last part of the study we considered the dependence of the switching process on the amplitude of the applied field. The measurements were performed at the field frequency of 10 Hz. The results observed at different experimental geometries are very similar. We present the results obtained at $\alpha=14°$. Figure 7 shows the temporal dependence of $P_{2\omega}$ at several field amplitudes starting from the amplitude of 357 V/cm, which corresponds to the field just above the critical field E_c, to 1714 V/cm. The asymmetric behavior of $P_{2\omega}$ with respect to the field sign change arises because at $\alpha=14°$

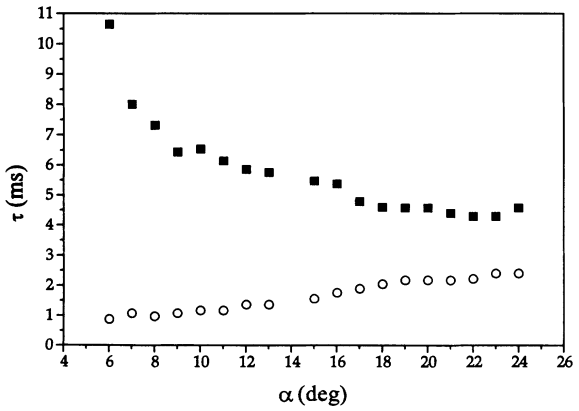

FIG. 5. The dependence of the delay time τ of the transient SHG peak on the incident angle α of the fundamental beam for the case of + to − sign change (squares) and for the case of − to + sign change (circles).

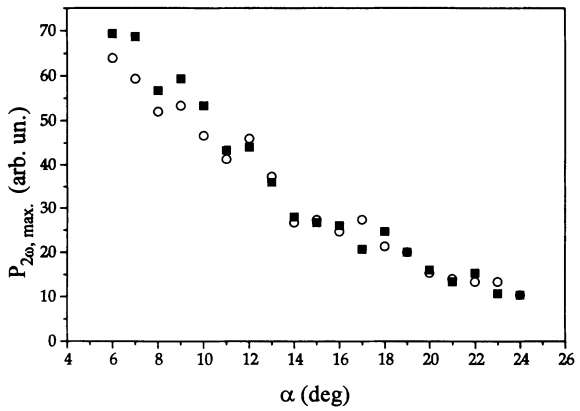

FIG. 6. The dependence of the height $P_{2\omega,\max}$ of the transient SHG peak on the incident angle α of the fundamental beam. The squares denote the data corresponding to the + to − sign change and the circles denote the data corresponding to the − to + sign change.

the direction of the optical beam in the sample is asymmetric with respect to the two equilibrium orientations of the director on the tilt cone.

The increase of the applied field amplitude decreases the delay time of the transient SHG peaks. This relation is depicted in Fig. 8, which shows the dependence of the inverse delay time $1/\tau$ on the field amplitude for both kinds of sign changes. The delay time of the peak following the + to − sign change decreases inversely proportionally to the field, while the behavior of the delay time of the peak following the − to + sign change is more complicated.

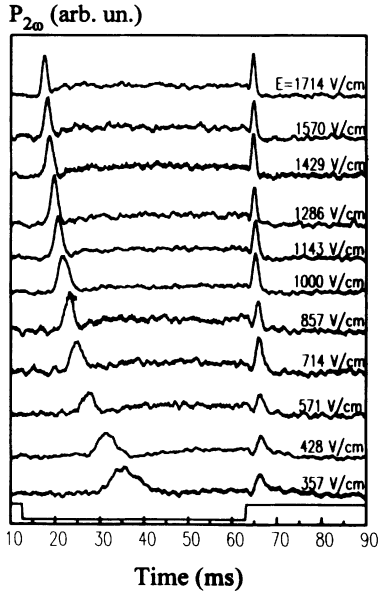

FIG. 7. Temporal dependence of the SHG at different amplitudes of the square wave form field measured at $\alpha=14°$. The temporal dependence of the field is marked in the bottom of the figure.

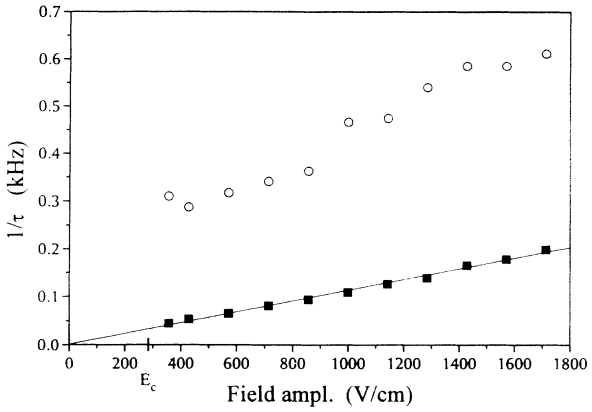

FIG. 8. The dependence of the inverse delay time $1/\tau$ of the transient SHG peak on the amplitude of the square wave form field for the case of + to − sign change (squares) and for the case of − to + sign change (circles). The solid line is the fit to the linear dependence of Eq. (10).

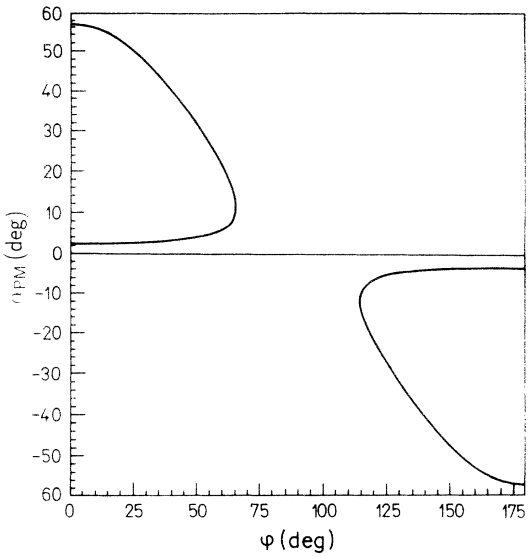

FIG. 9. The dependence of the phase matching direction α_{PM} on the phase angle φ of the director on the tilt cone in the model in which the molecules uniformly rotate on the tilt cone over the whole illuminated sample region.

IV. DISCUSSION

The variation of the PM direction with the frequency of the modulating field is assumed to be the consequence of the inequilibrium molecular configuration within the cell. We conclude from the SHG response at the frequency of 0.05 Hz that the full 180° reorientation of the molecular director between its two equilibrium positions on the tilt cone takes around 5 s. If the field changes its sign in time intervals shorter than 5 s the director never reaches the equilibrium states, but is rather flipping between the two limiting intermediate positions on the tilt cone. The orientation of the material optical axes and the related PM directions shift in accordance with these intermediate states. The intermediate states explain also the phenomenon of the transient SHG peaks. The transient peaks appear due to the transient realization of the PM condition along the actual direction of the optical beams, which is related to the certain director position established for a short time during the reorientation.

The direction and the polarization of the transient SHG peaks are very different from what is expected for the uniform director reorientation, that is, when the director in the whole cell moves uniformly on one side of the tilt cone [26]. The discrepancy in the direction is evident from Fig. 9, which shows the calculated dependence of the *ee-o* PM direction α_{PM} on the phase angle φ of the director on the tilt cone. In this calculation the SCE9 was assumed to be a homogeneous uniaxial material with the principal refractive indices $n_o(\omega)=1.52$, $n_e(\omega)=1.69$ at the fundamental frequency and $n_o(2\omega)=n_o(\omega)+0.011$ at the second-harmonic frequency [25,27]. The value $\varphi=0°$ corresponds to the equilibrium director orientation in the positive dc field and the value $\varphi=180°$ corresponds to the equilibrium director orientation in the negative dc field. During the negative field intervals at high modulation frequencies the director attains a maximum value of $\varphi<180°$, so according to Fig. 9 the α_{PM} corresponding to the possible intermediate director orientations should shift from $\alpha=-2.5°$ to some values $\alpha<-2.5°$. The PM could even altogether disappear if the director stays within the gap from $\varphi\approx 65°\leftrightarrow 115°$. This is opposite to the situation observed in the experiments, where for the fast modulation the PM direction α_{PM} during the negative field intervals shifts from negative to positive values (Fig. 3). The other discrepancy with respect to the uniform reorientation is the polarization of the transient SHG peaks. In the case of the uniform reorientation the polarization of the phase matched second-harmonic light, which corresponds to the ordinary optical beam, should vary with φ so that it would be always perpendicular to the actual director orientation. In contrast to this the polarization of the second-harmonic light in our experiments was parallel to the y axis all the time. All these features suggest that some more complex nonuniform reorientation model has to be considered to explain the experimental results.

We propose a model in which reorientation takes place within numerous small domains. In this model the director in each domain moves on either side of the tilt cone (Fig. 10). The two kinds of domains are denoted as $\vec{n}_+$ and $\vec{n}_-$ domains. The observed material properties, such as no significant increase in the scattering of the fundamental beam or a very nice angular PM profile detected even during the fast modulation, show that the average size of the domains is considerably smaller than the optical wavelength λ. This means that despite the domains the FLC material remains homogeneous from the optical point of view. The light beam is affected by an average system with the C_2 symmetry along the y axis and an average director $\langle\vec{n}\rangle$ changing with φ as shown in Fig. 10. The $\langle\vec{n}\rangle$ is the projection of either $\vec{n}_+$ or $\vec{n}_-$ on the xz plane. An apparent tilt angle ϑ of the system, that is the angle between $\langle\vec{n}\rangle$ and the z axis, varies with φ as

$$\vartheta=\arctan(\tan\theta\cos\varphi)\ . \tag{1}$$

As the angle between the PM direction α_{PM} and the $\langle\vec{n}\rangle$

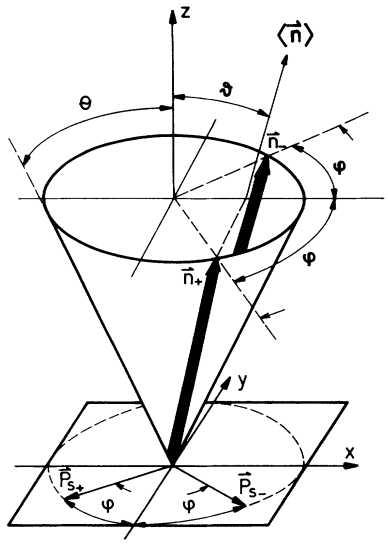

FIG. 10. The orientation of the director within the two kinds of domains ($\vec{n}_+$ and $\vec{n}_-$ domains) which are formed during the switching.

is quite constant, the α_{PM} shifts in accordance with the changing $\langle\vec{n}\rangle$.

The relation between the phase angle φ of the molecules on the tilt cone and the PM direction α_{PM} is calculated from the average material refractive index and its known color dispersion. Assuming that the two kinds of domains are present in equal proportions the average refractive index of the structure is obtained from the spatially averaged dielectric tensor:

$$\langle\varepsilon\rangle=\varepsilon_\perp\cdot\underline{1}+\tfrac{1}{2}\varepsilon_a(\vec{n}_+\otimes\vec{n}_++\vec{n}_-\otimes\vec{n}_-)\ , \tag{2}$$

were $\varepsilon_\perp$ is the dielectric constant in the direction perpendicular to the long molecular axis, $\varepsilon_a=\varepsilon_\parallel-\varepsilon_\perp$ is the dielectric anisotropy at the optical frequencies, and

$$\begin{aligned}\vec{n}_+&=(\sin\theta\cos\varphi,-\sin\theta\sin\varphi,\cos\theta)\ ,\\ \vec{n}_-&=(\sin\theta\cos\varphi,\sin\theta\sin\varphi,\cos\theta)\end{aligned} \tag{3}$$

are the intermediate orientations of the director on the tilt cone within the two kinds of domains. The average material structure is optically biaxial with the optical axes in the xz plane. The average principal refractive indices are

$$\begin{aligned}n_1&=\sqrt{\varepsilon_\perp}\ ,\\ n_2&=\sqrt{\varepsilon_\parallel-\varepsilon_a\sin^2\theta\sin^2\varphi}\ ,\\ n_3&=\sqrt{\varepsilon_\perp+\varepsilon_a\sin^2\theta\sin^2\varphi}\ .\end{aligned} \tag{4}$$

The relation between φ and α_{PM}, for the fundamental optical beam with the wave vector and polarization in the xz plane and the second-harmonic beam with polarization along the y axis, is

$$\alpha_{PM}(\varphi)=\arcsin\left[n_3(2\omega)\sin\left\{\vartheta-\arcsin\left[\pm\frac{n_2(\omega)}{n_3(2\omega)}\left[\frac{[n_1(\omega)]^2-[n_3(2\omega)]^2}{[n_1(\omega)]^2-[n_2(\omega)]^2}\right]^{1/2}\right]\right\}\right], \tag{5}$$

where $n_1(\omega)$, $n_2(\omega)$, and $n_3(2\omega)$ denote the average principal refractive indices at fundamental and at second-harmonic frequency. Taking again $[\varepsilon_\perp(\omega)]^{1/2}=n_o(\omega)=1.52$, $[\varepsilon_\parallel(\omega)]^{1/2}=n_e(\omega)=1.69$, and $n_o(2\omega)-n_o(\omega)=0.011$ [25], Eq. (5) results in the dependence $\alpha_{PM}(\varphi)$ shown in Fig. 11. As in Fig. 9 also in this figure the values $\varphi=0°$ and $\varphi=180°$ correspond to the equilibrium orientations of the director in the positive and in the negative dc field, respectively. The calculated dependence is in good agreement with the experimental results. For $\varphi=180°$ the α_{PM} is $-2.5°$. The α_{PM} increases with decreasing φ and at $\varphi=164°$ changes from negative to positive values. The value $\alpha_{PM}=+4°$ corresponds to the intermediate director reorientation with $\varphi=153°$. This orientation results in the PM profile determined at the end of the negative field intervals during the 10 Hz modulation. In the square wave form field with the frequency of 10 Hz the director is therefore flipping as $\varphi=27°\leftrightarrow153°$. The transient SHG peaks are related to some values of φ between these limits. Our model explains also why the polarization of the phase matched second-harmonic beam remains constant all the time during the switching. That is because in the system of numerous small domains the y axis coincides with one of the principal axes of $\langle\varepsilon\rangle$ [eigenvalue $n_3(2\omega)$] for all the values of φ.

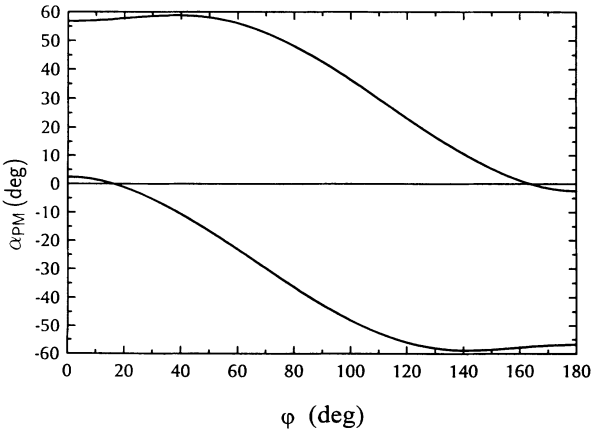

FIG. 11. The dependence of the phase matching direction α_{PM} on the phase angle φ of the director on the tilt cone in the model of the reorientation within numerous small domains.

The analysis of the transient PM data on the basis of relation (5) provides information on the dynamics of the switching process, that is, it gives the temporal dependence $\varphi(t)$. This dependence is obtained from the delay time data shown in Fig. 5 and is presented in Fig. 12. The axes are oriented so that the time t necessary for the molecules to reach different phase angles φ on the tilt cone is shown. The value $t=0$ corresponds to the mo-

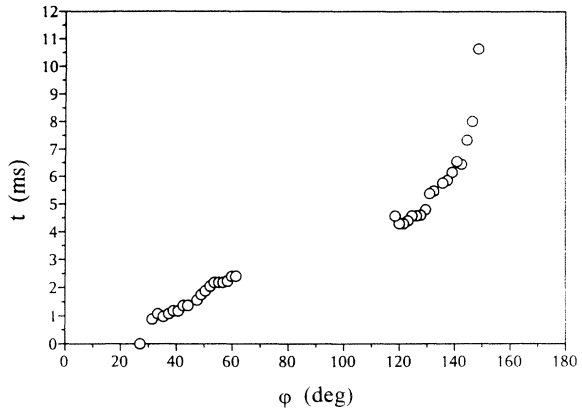

FIG. 12. The time t necessary for the director (either $\vec{n}_+$ or $\vec{n}_-$) to reach different phase angles φ on the tilt cone.

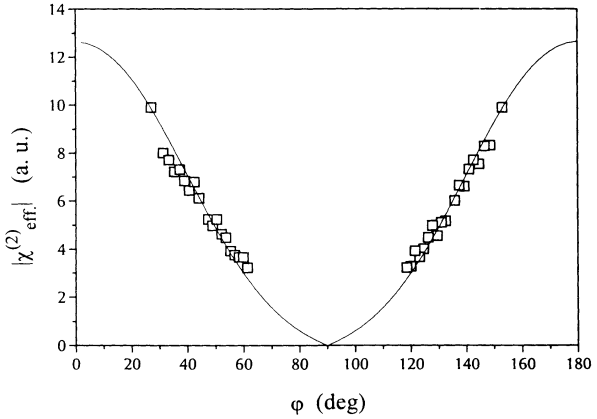

FIG. 13. The absolute value of the effective nonlinear optical susceptibility $|\chi^{(2)}_{\text{eff}}|$ of the multidomain structure as a function of the phase angle φ of the molecules on the tilt cone. The solid line is the fit of Eq. (9).

ment when the field sign is changed The values of t for $90°<\varphi<180°$ were calculated by direct comparison of $\tau(\alpha)$ data corresponding to the + to − sign change with the dependence $\alpha_{\text{PM}}(\varphi)$ shown in Fig. 11. The values for $0°<\varphi<90°$ were calculated from $\tau(\alpha)$ corresponding to the − to + sign change by replacing φ with $(180°-\varphi)$ on the graph in Fig. 11. By this procedure the two sets of experimental data were joined together into one diagram.

When the square wave form field with the frequency of 10 Hz is applied to the cell the director reorientation process starts at the initial phase angle $\varphi=27°$. The reorientation is then quite fast (ms time scale) until the phase angle $\varphi\approx140°$ is realized. At this value of φ a significant slowing down of the reorientation starts. In 50 ms (the end of the half of the square wave form field period) the position $\varphi=153°$ is reached. The field sign is then changed back to the previous value ($\varphi\rightarrow180°-\varphi$) and the complete reorientation process starts again. If the field periods are longer, the reorientation slowly proceeds toward $\varphi=180°$. This slow approach to the equilibrium orientation is observed in the field with the frequency of 0.05 Hz. At present there is no theory to describe the observed dynamical behavior. By comparing our results with the simplest uniform switching model one notices that the general shape of $t(\varphi)$ is quite similar to the case of uniform switching, but the interval of slow dynamics around $\varphi=180°$ is extended from a few degrees to a few tens of degrees [26].

The analysis of the height $P_{2\omega,\max}$ of the transient SHG peaks (Fig. 6) gives the relation between φ and the absolute value of the effective nonlinear optical susceptibility $|\chi^{(2)}_{\text{eff}}|\propto(P_{2\omega,\max})^{1/2}$ of the material. This relation is presented in Fig. 13. The $|\chi^{(2)}_{\text{eff}}|$ depends on $|\varphi-90°|$ and goes to zero for $\varphi=90°$. The quantitative dependence is again analyzed within the model of numerous small domains.

The nonlinear optical susceptibility of the domain structure is determined by the spatial average of the tensor of nonlinear optical susceptibility $\chi^{(2)}$. This is

$$\langle\chi^{(2)}\rangle=\tfrac{1}{2}(\chi^{(2)}_{+}+\chi^{(2)}_{-}) , \tag{6}$$

where $\chi^{(2)}_{+}$ and $\chi^{(2)}_{-}$ denote the tensors of nonlinear optical susceptibility within the $\vec{n}_+$ and within the $\vec{n}_-$ domains, respectively. Due to the C_2 symmetry of the average material structure only four of the ten independent components of the $\langle\chi^{(2)}\rangle$ differ from zero. These are $\langle\chi_{xzy}\rangle$, $\langle\chi_{xxy}\rangle$, $\langle\chi_{zzy}\rangle$, and $\langle\chi_{yyy}\rangle$. The components $\langle\chi_{ijk}\rangle$ are calculated by considering the explicit values of the nonlinear optical susceptibility of SCE9. In this FLC two of the susceptibility components strongly predominate. In the local coordinate system with $Z\|\vec{n}$ and $Y\|\vec{P}_s$ (where $\vec{P}_s$ denotes the spontaneous polarization in the Sm-C^* phase) these are χ_{ZZY} and χ_{YYY} [25]. By taking only these two components into account for the calculations the following relations result:

$$\begin{aligned}
&\langle\chi_{xzy}\rangle=\tfrac{1}{4}\chi_{ZZY}\sin2\theta\cos2\varphi ,\\
&\langle\chi_{xxy}\rangle=-\chi_{YYY}\sin^2\varphi\cos\varphi-\chi_{ZZY}\cos^2\theta\cos^3\varphi ,\\
&\langle\chi_{zzy}\rangle=-\chi_{ZZY}\sin^2\theta\cos\varphi ,\\
&\langle\chi_{yyy}\rangle=-\chi_{YYY}\cos^3\varphi-3\chi_{ZZY}\cos^2\theta\sin^2\varphi\cos\varphi .
\end{aligned} \tag{7}$$

In our experimental geometry we measure an effective nonlinear optical susceptibility $\chi^{(2)}_{\text{eff}}$ which is related to $\langle\chi_{ijk}\rangle$ as

$$\chi^{(2)}_{\text{eff}}=\langle\chi_{xxy}\rangle\cos^2\beta+\langle\chi_{zzy}\rangle\sin^2\beta-\langle\chi_{xzy}\rangle\sin2\beta , \tag{8}$$

where $\beta=\arcsin[\sin\alpha/n_3(2\omega)]$ is the angle between the optical beams and the z axis inside the cell (see also Fig. 1). By bearing in mind the facts that $(\chi_{ZZY}/\chi_{YYY})=2.7$ for the SCE9 and that $\beta<18°$ in all our experiments we finally look for the leading terms in Eq. (8), which are

$$|\chi^{(2)}_{\text{eff}}(\varphi)|\propto\cos\varphi+\cos^3\varphi(2.7\cos^2\theta-1) . \tag{9}$$

The fit of the experimental data to relation (9) is presented as the solid line in Fig. 13. The argeement between the model and the experiment is very good. The main feature of the figure, the decrease of the $|\chi^{(2)}_{\text{eff}}|$ when φ is approaching 90°, can also be qualitatively explained. At $\varphi=90°$ the apparent tilt angle ϑ of the molecules goes to zero and the symmetry is increased to $y\|D_2$. In this symmetry only the $\langle\chi_{xyz}\rangle$ component can be different from zero, while all the others vanish. For this reason

the SHG signal drastically decreases. At $\varphi=90°$ the nonlinear optical properties of the domain FLC structure become similar to that of the antiferroelectric Sm-C_A^* phase [28].

The dependence of the delay time τ of the transient SHG peaks on the amplitude of the applied field was studied at the incident angle α of 14°. In accordance with our model the transient PM at $\alpha=14°$ corresponds to the director reorientations $\varphi=27°\rightarrow\varphi=134.2°$ (+ to − sign change) and $\varphi=27°\rightarrow\varphi=45.8°$ (− to + sign change), respectively. To get some more quantitative ideas about the field effects on the reorientation dynamics in the domain structure, we compare our results with the most simple dynamic equation for the uniform switching

$$\gamma(\partial\varphi/\partial t)\cong P_s E\sin\varphi\ , \tag{10}$$

where γ is the rotational viscosity of the material. In the case of uniform switching the temporal dependence of φ scales as $(\gamma/P_s E)$ [26]. In accordance with the solution $t(\varphi)$ of Eq. (10) we calculate the value for γ corresponding to our measurements. The fit, which is presented as a solid line in Fig. 8, gives the value γ of 0.14 Pa s. The manufacturer of SCE9 (British Drug House Ltd.) specifies the viscosity of 0.40 Pa s. The difference between these two values may be understood as a measure of the discrepancy between the actual reorientation process and the uniform switching model.

V. CONCLUSION

Our measurements show that the reorientation of a thick homeotropic cell of FLC in transverse electric field proceeds via numerous domains, which are considerably smaller than the wavelength of visible light. The reorientation process, which at the beginning progresses on a ms time scale, becomes quite slow close to the equilibrium states. This slow response makes homeotropic cells less promising for applications for the SHG modulation as was expected in the literature. We have demonstrated that on the other hand a detailed study of the SHG is an exceptionally good method to resolve the complex dynamics of the switching. This is because the efficient phase matching geometry depends monotonically on the orientation of the director within the cell.

ACKNOWLEDGMENTS

The experiments were performed at European Laboratory for Nonlinear Spectroscopy (LENS) in Florence, Italy. One of the authors, I.D.O., is grateful to the Ministry of Science and Technology of Slovenia for supporting her stay in Florence and to the director of LENS, S. Califano, for providing the use of research facilities at LENS.

[1] M. A. Handschy and N. A. Clark, Appl. Phys. Lett. **41**, 39 (1982).
[2] H. Orihara and Y. Ishibashi, Jpn. J. Appl. Phys. **23**, 1274 (1984).
[3] Y. Ouchi, H. Takano, H. Takezoe, and A. Fukuda, Jpn. J. Appl. Phys. **26**, L21 (1987).
[4] Y. Ouchi, H. Takezoe, and A. Fukuda, Jpn. J. Appl. Phys. **26**, 1 (1987).
[5] W. Hartmann, Ferroelectrics **85**, 455 (1988).
[6] N. A. Clark and S. T. Lagerwall, Appl. Phys. Lett. **36**, 899 (1980).
[7] T. Tsuchiya, K. Ito, M. Isogai, and M. Odamura, Jpn. J. Appl. Phys. **25**, L27 (1986).
[8] J. E. Maclennan, M. A. Handschy, and N. A. Clark, Phys. Rev. A **34**, 3554 (1986).
[9] A. I. Allagulov, S. A. Pikin, and V. G. Chigrinov, Liq. Cryst. **5**, 1099 (1989).
[10] T. C. Chieu, Jpn. J. Appl. Phys. **30**, 747 (1991).
[11] J. W. Goodby, R. Blinc, N. A. Clark, S. T. Lagerwall, M. A. Osipov, S. A. Pikin, T. Sakurai, K. Yoshino, and B. Žekš, *Ferroelectric Liquid Crystals: Principles, Properties and Applications,* Vol. 7 of *Ferroelectricity and Related Phenomena,* edited by G. W. Taylor (Gordon and Breach, Philadelphia, 1991).
[12] F. Gießelmann and P. Zugenmaier, Liq. Cryst. **14**, 389 (1993).
[13] J. Etxebarria, M. A. Perez Jubindo, A. Ezcurra, and M. J. Tello, J. Appl. Phys. **63**, 4921 (1988).
[14] A. Jakli, L. Bata, and L. A. Beresnev, Mol. Cryst. Liquid Cryst. **177**, 43 (1989).
[15] L. A. Beresnev and L. M. Blinov, Ferroelectrics **92**, 729 (1989).
[16] M. Ozaki, A. Tagawa, Y. Sadohara, S. Oda, and K. Yoshino, Jpn. J. Appl. Phys. **30**, 2366 (1991).
[17] M. Utsumi, T. Gotou, K. Daido, M. Ozaki, and K. Yoshino, Jpn. J. Appl. Phys. **30**, 2369 (1991).
[18] A. N. Vtyurin, V. P. Ermakov, B. I. Ostrovskii, and V. F. Shabanov, Phys. Status Solidi B **107**, 397 (1981).
[19] N. M. Shtykov, M. I. Barnik, L. A. Beresnev, and L. M. Blinov, Mol. Cryst. Liq. Cryst. **214**, 379 (1985).
[20] K. Yoshino, S. Kishio, M. Ozaki, A. Yukoatani, T. Sasaki, and C. Yamanaka, Technol. Rep. Osaka Univ. **37**, 283 (1987).
[21] A. Taguchi, Y. Ouchi, H. Takezoe, and A. Fukuda, Jpn. J. Appl. Phys. **30**, L997 (1989).
[22] M. Ozaki, M. Utsumi, T. Gotou, K. Daido, and K. Yoshino, Jpn. J. Appl. Phys. **30**, L1569 (1991).
[23] M. Ozaki and K. Yoshino, Jpn. J. Appl. Phys. **28**, L1830 (1989).
[24] I. Drevenšek, R. Torre, and M. Čopič, Mol. Cryst. Liq. Cryst. (to be published).
[25] J. Y. Liu, M. G. Robinson, K. M. Johnson, and D. Doroski, Opt. Lett. **15**, 267 (1990).
[26] X. Jiu-Zhi, M. A. Handschy, and N. A. Clark, Ferroelectrics **73**, 305 (1987).
[27] See, for example, A. Yariv, *Quantum Electronics,* 2nd ed. (Wiley, New York, 1975).
[28] T. Fujioka, K. Kajikawa, H. Takezoe, A. Fukuda, T. Kusumoto, and T. Hiyama, Jpn. J. Appl. Phys. **32**, 4589 (1993).